

ULTRA DEEP SUB-KPC VIEW OF NEARBY MASSIVE COMPACT GALAXIES

IGNACIO TRUJILLO^{1,2}

Instituto de Astrofísica de Canarias, Vía Láctea s/n, 38200 La Laguna, Tenerife, Spain

ELEAZAR R. CARRASCO

Gemini Observatory/AURA, Southern Operations Center, Casilla 603, La Serena, Chile

AND

ANNA FERRÉ-MATEU²

Instituto de Astrofísica de Canarias, Vía Láctea s/n, 38200 La Laguna, Tenerife, Spain

Draft version March 18, 2019

ABSTRACT

Using Gemini North telescope ultra deep and high resolution (sub-kpc) K-band adaptive optics imaging of a sample of 4 nearby ($z \sim 0.15$) massive ($\sim 10^{11} M_{\odot}$) compact ($R < 1.5$ kpc) galaxies, we have explored the structural properties of these rare objects with an unprecedented detail. Our surface brightness profiles expand over 12 magnitudes in range allowing us to explore the presence of any faint extended envelope on these objects down to stellar mass densities $\sim 10^6 M_{\odot}/\text{kpc}^2$ at radial distances of ~ 15 kpc. We find no evidence for any extended faint tail altering the compactness of these galaxies. Our objects are elongated, resembling visually S0 galaxies and have a central stellar mass density well above the stellar mass densities of objects with similar stellar mass but normal size in the present universe. If these massive compact objects will eventually transform into normal size galaxies, the processes driving this size growth will have to migrate around $2-3 \times 10^{10} M_{\odot}$ stellar mass from their inner ($R < 1.7$ kpc) region towards their outskirts. Nearby massive compact galaxies share with high- z compact massive galaxies not only their stellar mass, size and velocity dispersion but also the shape of their profiles and age of their stellar populations. This makes these singular galaxies unique laboratories to explore the early stages of the formation of massive galaxies.

Subject headings: Galaxies: Evolution, Galaxies: Formation, Galaxies: Spiral, Galaxies: Structure
Galaxies: Photometry

1. INTRODUCTION

Following the discovery (Daddi et al. 2005; Trujillo et al. 2006) that massive spheroid-like galaxies ($M_{\star} \gtrsim 10^{11} M_{\odot}$) at $z \gtrsim 1$ were significantly more compact than their local equivalent counterparts, there has been some efforts exploring whether any single of these galaxies can be found in the nearby Universe (Trujillo et al. 2009; Taylor et al. 2009; Valentinuzzi et al. 2010; Shih & Stockton 2011). According to some theoretical models (Hopkins et al. 2009a) it would be possible that some of the massive compact high redshift galaxies should have survived untouched since their formation epoch. Consequently, the discovery of a population of nearby old compact massive galaxies would open the possibility of exploring the galaxy formation mechanisms of the early universe in exquisite detail. So far, the amount of nearby massive galaxies with sizes ($\lesssim 1.5$ kpc) similar to the median value found at $z \gtrsim 2$ (e.g. Trujillo et al. 2007; Buitrago et al. 2008) represents only a tiny fraction ($\sim 0.03\%$) of the massive objects in the nearby universe ($z < 0.2$; Trujillo et al. 2009). Moreover, contrary to theoretical expectations, the nearby compact massive galaxies have average stellar ages which are relative young (~ 2 Gyr), more younger than the age expected if they

were relics from an early formation epoch. In this sense, present day massive compact galaxies, more than remnants from an early epoch, resemble almost perfect counterparts of the massive galaxy population found at $z \sim 2$: they have similar stellar masses, sizes and ages (Trujillo et al. 2009; Ferré-Mateu et al. 2012). What is currently missed though, is an in-depth analysis of the morphological properties of the nearby massive compact population.

Detailed analysis of the stellar mass density profiles of massive compact galaxies at high redshift (Bezanson et al. 2009; Hopkins et al. 2010; van Dokkum et al. 2010; Carrasco et al. 2010) show that these objects have a moderate excess of stellar mass density at their centers and a significant lack of stars in their outer regions. In fact, it is this lack of a tail in their stellar profiles what is making them to look so compact. The studies of the morphological properties of the nearby massive galaxy population have been seriously limited as the presently available imaging of these objects is based on ground based observations (with a typical seeing of ~ 1 arcsec or equivalent to ~ 2.6 kpc at $z = 0.15$). This has prevented a detailed analysis of the inner region of these galaxies. Also, the outer parts of these galaxies have not been studied in detail. For that reason, a deep sub-kpc view of these galaxies would be of great help to put these galaxies into context within the local massive galaxy population. Under the assumption that these massive compact galaxies are similar objects to those found at high redshift (i.e. both in structural and stellar population

trujillo@iac.es

¹ Ramón y Cajal Fellow

² Departamento de Astrofísica, Universidad de La Laguna, E-38205 La Laguna, Tenerife, Spain

properties) the unprecedented detailed analysis that can only be conducted in nearby galaxies will allow us to constrain the different evolutionary paths that transform these galaxies into the massive "normal sized" galaxy population. In particular, with this work we would like to answer the following questions: what is the morphological nature of the massive galaxies in their primitive state: disk or spheroidal? Does the compactness nature of these objects an artifact due to the missing of light in the outer regions? In this paper, we present ultra-deep high resolution K-band imaging obtained with the Gemini North telescope of a sample of four nearby massive compact galaxies from the sample presented in Trujillo et al. (2009). We will show that the most common nature of the nearby massive compact galaxies is disk and that there is not any evidence indicating that their stellar mass density profiles have an extended outer envelope biasing their size estimates. In what follows, we adopt a cosmology of $\Omega_m=0.3$, $\Omega_\Lambda=0.7$ and $H_0=70$ km s^{-1} Mpc $^{-1}$.

2. THE DATA

The galaxies studied here are a sub-sample of the collection of nearby compact massive galaxies compiled by Trujillo et al. (2009). The original sample contains 48 bona-fide compact massive galaxies taken from the New York University Value-Added Galaxy Catalog from the SDSS Data Release 6 (Blanton et al 2005; NYU from now onwards). Our galaxies have a mean redshift of 0.16, a mean effective radius of ~ 1.3 kpc with no detected signatures of AGN in their spectra which might affect the size determination, and a mean stellar mass of $\sim 9.2 \times 10^{10} M_\odot$ (Chabrier 2003 Initial Mass Function).

The high spatial resolution imaging presented here was obtained with the Gemini North telescope using the Near-Infrared Imager and Spectrometer (NIRI; Hodapp et al. 2003) with the ALTAIR/LGS (Laser Guide Star) adaptive optics systems (Herriot et al. 2000, Boccas et al. 2006). ALTAIR requires a relatively bright star ($\lesssim 18$ mag in R-band) in the proximity of the target object (within $17''$) to obtain a good Strehl correction. We got time to explore four galaxies of the Trujillo's sample that satisfy this criteria. The final galaxy sample has Adaptive Optic (AO) tip-tilt stars with magnitudes between 15.8 and 17.9 in R-band located within $16''$ of the main target.

The galaxies were observed during the first semester of 2010, in queue mode, using the K ($2.2 \mu\text{m}$) filter and NIRI f/14 camera, which provides a field of view of $51''.1 \times 51''.1$ with pixel scale of $0''.0488$ on side onto a 1024×1024 ALADDIN InSb array. In addition, standard stars for photometric calibration were observed before or after our galaxies. The standard stars were used to determine the photometric zero points and monitor the image quality of the observations. Throughout the standard stars and the field stars presented in our observations we determined the effective FWHM of our observations. From standard stars, the effective FWHM varied between $0''.11$ and $0''.13$ (note that the photometric standard stars have always the maximum Strehl corrections because they are used as AO tip/tilt star). From field stars, the effective FWHM was between $0''.16$ and $0''.24$ varying with the stellar magnitude, and the location of the star relative to the galaxy of interest. The

galaxy SDSS-J153934.07+441752.2 was observed in separate nights (see Table 1), but at similar airmass. For galaxy J120032.46+032554.1 only 27 images of 60 sec were observed (half of the planned observations). Despite this reduction, the combined image for this galaxy is still very deep allowing us to reach faint surface brightness.

The data were processed following the standard procedures for near-infrared imaging using the NIRI/Gemini IRAF package v1.10. Normalized flat field images were constructed from flat images observed with the Gemini Calibration unit (GCAL) with the shutter closed (lamps off) and shutter open (lamps on). Dark images observed at the end of each night and flat field images (lamp off) were used to construct a bad pixel mask with bad and hot pixels. The sky images were constructed from the raw science images by identifying objects in each frame, masking them out, and averaging the remaining good pixel (the images were observed with a $3'' \times 3''$ mosaic pattern). The raw science images were then processed by subtracting the sky on a frame-by-frame basis and divided by the normalized flat field images. Finally, the processed images were registered to a common pixel position and median combined. The final images have a field of view of $39''.5 \times 39''.5$. The images of our four galaxies are shown in Figure 1.

Photometric calibrations were derived using the UKIRT Mauna Kea Observatories JHKL'M Standard Stars FS 132 (s860-d), FS 152 (p460-e) and P272-D (Leggett et al. 2006) and the P064-D faint standard star (Persson et al 1998). Given that only one standard star was observed for each galaxy (before or after), we have used an average value for the extinction of $k_K = 0.052 \pm 0.028$ from Leggett et al. (2006). Table 1 lists all observational parameters for our NIRI observations. Since we use an average value for the extinction coefficient, the estimated error in the photometric calibration will be driven by the uncertainty in the correct value of the extinction coefficient for the night of observation. Hence, we estimated the error by summing in quadrature the median error of the aperture photometry, the error of the standard catalog and the median error of the extinction coefficient. The error varied between 0.03 mag and 0.05 mag, depending on the star. For each galaxy, the adopted zero point is listed in the column (7) of Table 1. The values were transformed from the Vega system to the AB system using the relation $K_{AB} - K_{Vega} = 1.91$ mag.

3. ANALYSIS

A visual inspection of the nearby compact massive galaxies shown in Fig. 1 indicates that the most common morphology of our objects is disk. In fact, two objects (SDSS J103050.53+625859.8 and SDSS J120032.46+032554.1) visually resemble S0 galaxies viewed in edge-on projection. The other two galaxies (SDSS J153934.07+441752.2 and SDSS J212052.74+110713.1) have a more distorted morphology but still are compatible with being S0 galaxies with a lower inclination (see also Valentinuzzi et al. 2010). On what follows, we make a quantitative analysis of the structural properties of the nearby compact massive galaxies.

3.1. *K-band surface brightness profiles*

In Fig. 2 we show circular aperture K-band surface brightness profiles of our compact galaxies. Although our galaxies have a clear elongation, circular apertures are taken to allow a direct comparison with the circular averaged profiles of "normal-sized" galaxies as we will show later. To create our profiles we followed the same technique explained in Pohlen & Trujillo (2006). Briefly, we obtain first the surface brightness profile of the galaxy up to large distances. Then we estimate the sky contribution in those regions outside the galaxy where the profile is flat and we remove (add) this value from (to) the images. After doing that, we calculate again the surface brightness profiles of these galaxies.

For most of our galaxies we can explore the surface brightness down to ~ 27 mag/arcsec². This implies probing around 12 magnitudes from the peak of the surface brightness profile down to our last observed point. This extraordinary depth allow us to investigate whether there is any evidence for any extra hidden (halo-like) component in our galaxies which due to its faintness could not have been observed in previous shallower images of these objects. We can consequently address whether previous works have incorrectly measured the sizes of these objects towards lower values.

We have fitted our profiles with a single Sérsic model to compare the sizes we get from our images in relation to those obtained in previous shallower and worst resolution SDSS data (Trujillo et al. 2009). We avoided in this fitting those regions of the galaxies more severely affected by the PSF. This means we only take those points beyond the FWHM of our PSF (this distance is indicated by a vertical dashed line in Fig. 2). The effective radii and Sérsic indices we got are shown in Table 2. We explored whether our results were affected by this particular radial range of exploration. To do that we repeat our fitting only taking the points outside 2 times the FWHM. Our estimates remained very well constrained with changes in the effective radius below 15% and for the Sérsic index less than 11%. This robustness is due to the extreme depth of our images.

We can now compare these values against the sizes obtained using SDSS imaging. In Trujillo et al. (2009) we got the following values: 1.42 kpc (103050.5), 1.31 kpc (120032.4), 1.11 kpc (153934.0) and 1.38 kpc (212052.7). We can see that the agreement with the present much deeper and higher resolution data is excellent with differences less than 7%. This is an indirect proof that there is not any hidden component in these massive nearby compact galaxies which is altering the size of the objects. The main novelty that the present deep data allow us to explore is the shape of these galaxies. We observe that these objects are well fitted with moderately low Sérsic indices ($2 < n < 4$) values. The absence of large Sérsic indices is again against the idea that there is a missing faint component surrounding these objects.

3.2. *Stellar mass density profiles*

In order to understand the building of the massive galaxies it is worth comparing the stellar mass density profiles of the compact population against the mass distribution of galaxies of a similar mass but with normal sizes. We have transformed our observed K-band surface

brightness profiles into stellar mass density profiles using the total stellar masses measured in Blanton et al. (2005) listed in Table 2. We have assumed that the stellar mass to light ratio is constant along the radial distance of the galaxy. The outcome of this exercise is presented in Fig. 3.

To build the stellar mass density profiles of the "normal-sized" galaxies used as a reference, we took the structural parameters (Sérsic index n , effective radius r_e and stellar mass M_*) of all the galaxies in the NYU catalogue (Blanton et al. 2005) with $0.8 < M_* < 1.2 \times 10^{11} M_\odot$ and $0.1 < z < 0.2$. These NYU structural parameters were retrieved from profiles obtained using circular apertures. To facilitate the comparison with our profiles, we divided the NYU galaxies into two different categories: disk-like ($n < 2.5$) and spheroid-like ($n > 2.5$). We find that the average disk-like massive galaxy within the NYU sample at those redshifts has $M_* = 0.95 \times 10^{11} M_\odot$, $n = 2$ and $r_e = 5.7$ kpc. On the other hand, the average spheroid-like object has $M_* = 0.98 \times 10^{11} M_\odot$, $n = 4$ and $r_e = 4.7$ kpc.

Once we obtained these average galaxy profiles, the representative regions of each galaxy category were build using all the galaxies in the NYU sample within the above stellar mass range and redshift interval whose central stellar mass densities were within the 68% of the distribution centered around the mean value.

From the comparison of the stellar mass density profiles of the compact galaxies with those of "normal-sized" objects (Fig. 3) is straightforward to conclude that the compact galaxies do not resemble neither of the two categories. Although visually the elongation of the compact galaxies would suggest that these objects are more likely disks, the shape of these profiles are closer to those considered as spheroids in the local universe. It is easy to see that there is an excess of mass at the center of the compact galaxies and a lack of stars (starting mainly around 3 kpc) in the outer regions. The deep profiles that we present here undoubtedly show that nearby massive compact galaxies do not have an extended outer component and, consequently, are genuinely compact.

An interesting exercise that can be conducted is to estimate the amount of stellar mass within the inner ($R < 3$ kpc) region of the compact galaxies and compare this to the "normal-sized" objects. In the case of the compact galaxies we find that the stellar mass fraction inside 3 kpc ranges from 0.72 (in the case of 212052.7) up to 0.89 (for 153934.0). In the case of "normal-sized" objects these fractions are significantly lower: 0.27 for disk-like objects and 0.38 in the case of spheroids. This implies that there is ~ 2 times more stellar mass inside 3 kpc in the case of the compact massive galaxies than in objects of the same stellar mass but normal size. This difference in stellar mass implies that one would expect a much larger central velocity dispersion in the case of compact galaxies compared to normal galaxies with equivalent stellar mass. A crude estimation (following the virial theorem expectation) suggests that this increase should be of the order of $\sqrt{2}$ as there is a factor of 2 more stellar mass in the central regions. Are these expectations in agreement with observations? In Trujillo et al. (2009) we found that the average central velocity dispersion of $10^{11} M_\odot$ galaxies according to SDSS was 180 km/s. Our massive compact galaxies have (see Table 2) an average $\sigma = 243$

km/s. This is 1.35 larger than the value found in normal galaxies of the same stellar mass and fits very well with the virial $\sqrt{2}$ expectation. This is another indirect proof of the larger stellar mass densities than massive compact galaxies have in their centers.

4. DISCUSSION

4.1. *Can massive compact galaxies be transformed into the core of giant ellipticals?*

A popular idea is that massive compact galaxies at high- z will end being the central part of present day most massive objects (Bezanson et al. 2009; Hopkins et al. 2009b). This scenario is supported by many indirect observational evidences as the progressive growth of the wings of the profiles of the massive galaxies with time (van Dokkum et al. 2010), the larger velocity dispersion of the massive galaxies at high- z (~ 1.5 times larger) compared to equally massive objects today (e.g. Cenarro & Trujillo 2009, Cappellari et al. 2009, Onodera et al. 2010, Newman et al. 2010, van de Sande et al. 2011), the similar number density ($\sim 2 \times 10^{-4} \text{ Mpc}^{-3}$) between $10^{11} M_{\odot}$ massive compact galaxies at high- z and today ~ 2 times more massive objects (van Dokkum et al. 2010, Cassata et al. 2011, Buitrago et al. 2012), the expected mass growth by a factor of ~ 2 of the massive galaxies with time expected theoretically (Naab et al. 2009, Sommer-Larsen & Toft 2010, Oser et al. 2012) and suggested by the observations (see e.g. Trujillo et al. 2011). In this sense, it is natural to compare our stellar mass density profiles with the profiles of normalized objects in the local universe but with a stellar mass twice the ones found for the local massive compact galaxies. The unprecedented resolution of our profiles allow us to see whether there is any change at sub-kpc level in the structure of these objects. In particular, we are interested on estimating how the growing processes that could eventually bring the compact galaxies into the core of more massive objects affect their inner regions. Moreover, we would like to quantify which number of stars should migrate during such transformation towards the outskirts of these objects.

In Fig. 4 (left panel) we show the comparison between the stellar mass density profiles of our nearby compact massive galaxies against objects with normal sizes but 2 times more massive. The nearby massive compact galaxies are clearly more dense at the center than the objects they will potentially be transformed in the future. That implies that the transformation from one class to another should imply a significant migration of the stars from the center of the compact galaxies towards their outer regions. The stellar mass density of both normalized and compact galaxies are similar at $R=1.7$ kpc. We can consequently estimate which is the excess of stellar mass of the compact galaxies compared to the other objects within this radius. We find that compact galaxies have $\sim 3 \times 10^{10} M_{\odot}$ more mass than a disk-like normal size galaxy and $\sim 2 \times 10^{10} M_{\odot}$ more mass than a spheroid object within 1.7 kpc. That means such amount of stellar mass should be relocated outwards of 1.7 kpc after the evolution of the compact galaxy into a larger size object. This enormous evolution of the inner region of the compact galaxies is expected in a minor merging scenario (see e.g. Fig. 3 of Oser et al. 2012). Both compact massive

galaxies and the larger objects have the same amount of stellar mass ($\sim 8 \times 10^{10} M_{\odot}$) within ~ 5 kpc. This suggests that the processes responsible of the growth of the galaxies locate most of the new assembled stars ($\sim 10^{11} M_{\odot}$) beyond that radius.

4.2. *Distant and nearby massive compact galaxies*

An interesting aspect that we can address with our data is whether our stellar mass density profiles resemble those of equally massive compact galaxies at $z \sim 2$. Contrary to what we find in the local universe, compact massive galaxies were very common at those redshifts. Consequently, if we prove that our nearby massive compact objects are similar in structure to their high- z counterparts, this would favor the idea that these objects share a similar formation origin. So far, not only the size, stellar mass and velocity dispersion of the nearby compact galaxies are the same than their equivalent high- z objects but there is some evidence implying that the compact nearby galaxies are young too (with an age $\sim 1-2$ Gyr; Trujillo et al. 2009, Ferré-Mateu et al. 2012). This age is equivalent to the age of the compact objects found at high- z (e.g. Kriek et al. 2009). The question that we address in this paper is whether the distribution of the stars in the nearby compact massive galaxies also follow a similar shape to the ones found at high- z . This is shown in Fig. 4 (right panel).

The objects that we have used to compare with our compact galaxies are the massive compact galaxies from the sample of Szomoru et al. (2012) at $z \sim 2$. This is a collection of 12 galaxies observed with the HST WFC3 as part of the CANDELS GOODS-South. The high- z objects have a median stellar mass of $8.3 \times 10^{10} M_{\odot}$ (Kroupa IMF) and a median size of 0.84 kpc. The high- z profiles presented in Szomoru et al. (2012) are deconvolved so we can have a better idea of how the profiles at high- z look in their inner ($R < 1$ kpc) regions. We can see that the agreement between the nearby and high- z compact galaxies is excellent.

It is evident from the images shown in Fig. 1 that our galaxies are elongated. We have measured their axis ratio using the ELLIPSE from IRAF. The axis ratio measured in the outer regions is shown in Table 2. Is there any evidence about a similar elongated shape for the compact massive galaxies at high- z ? van der Wel et al. (2011) and Buitrago et al. (2012) have addressed this issue and find that this is the case. Most of high- z massive galaxies at high- z have elongated shapes too. Summarizing, nearby massive compact galaxies are almost exact copies of the high- z massive compact galaxies suggesting that their detailed study can shed light on the formation of the first massive galaxies assembled in the Universe.

5. CONCLUSIONS

Using ultra-deep imaging at a sub-kpc resolution of a sample of 4 nearby massive compact galaxies, we have shown unequivocally that these objects are genuinely compact with no evidence of an extended faint component altering their size estimate. These nearby massive compact galaxies have an elongated shape resembling the structure of S0 objects. Their stellar mass density profiles are significantly more dense in their inner regions than any galaxy with similar stellar mass and normal size in the local universe.

Nearby massive compact galaxies share a large number of properties with massive compact galaxies in the distant universe: same stellar mass, size, shape, velocity dispersion and very likely the age of their stellar populations. Contrary to high- z compact massive galaxies which were very common among the family of massive galaxies at $z \sim 2$, nearby massive compact galaxies are a tiny fraction of the family of massive galaxies today. It still unclear whether the nearby compact massive galaxies are relics of that epoch (which have had a recent burst of star formation that has rejuvenated their ages) or whether they are truly young galaxies recently assembled. Undoubtedly, the study of these rare nearby objects open the possibility of exploring in exquisite detail the early stages of massive galaxy formation.

I.T. is Ramón y Cajal Fellows of the Spanish Ministry of Science and Innovation. This work has been supported by the Programa Nacional de Astronomía y Astrofísica of the Spanish Ministry of Science and Innovation under grant AYA2010-21322-C03-02. Based on observations obtained at the Gemini Observatory, which is operated by the Association of Universities for Research in Astronomy, Inc., under a cooperative agreement with the NSF on behalf of the Gemini partnership: the National Science Foundation (United States), the Science and Technology Facilities Council (United Kingdom), the National Research Council (Canada), CONICYT (Chile), the Australian Research Council (Australia), Ministério da Ciência, Tecnologia e Inovação (Brazil) and Ministerio de Ciencia, Tecnología e Innovación Productiva (Argentina). Program ID: GN-2010A-Q-24.

Gemini-SouthNIRI/Altair

REFERENCES

- Ayres, T. R. 2005, 13th Cambridge Workshop on Cool Stars, Stellar Systems and the Sun, 560, 419
- Beasley, M. A., Cenarro, A. J., Strader, J., & Brodie, J. P. 2009, *AJ*, submitted
- Bezanson, R., van Dokkum, P. G., Tal, T., Marchesini, D., Kriek, M., Franx, M. & Coppi, P., 2009, *ApJ*, 697, 1290
- Blanton, M. R., et al. 2005, *AJ*, 129, 2562
- Blanton, M. R., & Roweis, S. 2007, *AJ*, 133, 734
- Boocas, M., et al., 2006, *SPIE*, 6272, 114
- Bruzual, G., & Charlot, S. 2003, *MNRAS*, 344, 1000
- Buitrago, F., Trujillo, I., Conselice, C. J., Bouwens, R. J., Dickinson, M., & Yan, H. 2008, *ApJ*, 687, L61 (B08)
- Buitrago, F., Trujillo, I., Conselice, C. J., Haeussler, B., 2012, arXiv:1111.6993
- Cappellari, M., et al., 2009, *ApJ*, 704, L34
- Cardiel, N. 1999, Ph.D. Thesis, Universidad Complutense de Madrid
- Carrasco, E. R., Conselice, C. J., Trujillo, I., 2010, *MNRAS*, 405, 2253
- Cassata, P. et al., 2011, *ApJ*, 743, 96
- Chabrier, G. 2003, *PASP*, 115, 763
- Cenarro, A. J., Trujillo, I., 2009, *ApJ*, 696, 43
- Cimatti et al. 2008 *A&A*, 482, 21 (C08)
- Daddi, E., et al. 2005, *ApJ*, 626, 680
- Damjanov, I., et al. 2008, arXiv:0807.1744
- di Serego Alighieri, S., et al. 2005, *A&A*, 442, 125
- Fan, L., Lapi, A., De Zotti, G., & Danese, L. 2008, *ApJ*, 689, L101
- Ferré-Mateu, A., et al., *MNRAS*, submitted
- Gregg, M. D., et al. 2004, *Bulletin of the American Astronomical Society*, 36, 1496
- González, J. J., 1993, PhDT, University of California
- Heap, S. R., & Lindler, D. J. 2007, *From Stars to Galaxies: Building the Pieces to Build Up the Universe*, 374, 409
- Herriot, G., et al., 2000, *SPIE*, 4007, 115
- Hills, J. G. 1980, *ApJ*, 235, 986
- Hodapp, K.W. et al., 2003, *PASP*, 115, 1388
- Hopkins, P. F., Hernquist, L., Cox, T. J., Keres, D., & Wuyts, S. 2009a, *ApJ*, 691, 1424
- Hopkins, P. F., Bundy, K., Murray, N., Quataert, E., Lauer, T. R., Ma, C.-P., 2009b, 398, 898
- Hopkins, P. F., Bundy, K., Hernquist, L., Wuyts, S., Cox, T. J., 2010, *MNRAS*, 401, 1099
- Khochfar, S., & Silk, J. 2006, *ApJ*, 648, L21
- Kriek, M., van Dokkum, P. G., Labb, I., Franx, M. Illingworth, G. D., Marchesini, D., Quadri, R. F., 2009, *ApJ*, 700, 221
- Leggett, S. K., et al., 2006, *MNRAS*, 373, 781
- Longhetti, M., et al. 2007, *MNRAS*, 374, 614
- Naab, T., Johansson, P. H., Ostriker, J. P., 2009, *ApJ*, 699, L178
- Newman, A. B.; Ellis, R. S., Treu, T., Bundy, K., 2010, *ApJ*, 717, L103
- Onodera, M., et al. 2010, *ApJ*, 715, L60
- Oser, L., Naab, T., Ostriker, J. P., Johansson, P. H., 2012, *ApJ*, 744, 630
- Persson, S. E., Murphy, D. C., Krzeminiski, W., Roth, M., & Rieke, M. J., 1998, *AJ*, 116, 2475
- Pohlen, M., & Trujillo, I., 2006, *A&A*, 454, 759
- Saracco, P., Longhetti, M., & Andreon, S. 2009, *MNRAS*, 392, 718
- Sargent, W. L. W., Schechter, P. L., Bokkenberg, A., & Shorridge, K. 1977, *ApJ*, 212, 326
- Sersic, J. L. 1968, Cordoba, Argentina: Observatorio Astronomico, 1968,
- Shih, H.-Y. & Stockton, A., *ApJ*, 733, 45
- Sommer-Larsen, J. & Toft, S., 2010, *ApJ*, 721, 1755
- Szomoru, D., Franx, M., van Dokkum, P. G., 2012, *ApJ*, submitted, arXiv1111.3361
- Taylor, E., Franx, M., Glazebrook, K., Brinchmann, J.; van der Wel, A. & van Dokkum, P. G., *ApJ*, 720, 723
- Toft, S., et al. 2007, *ApJ*, 671, 285
- Trujillo, I., et al. 2006, *MNRAS*, 373, L36
- Trujillo, I., Conselice, C. J., Bundy, K., Cooper, M. C., Eisenhardt, P., & Ellis, R. S. 2007, *MNRAS*, 382, 109
- Trujillo, I., Cenarro, A. J., de Lorenzo-Caceres, A., Vazdekis, A., de la Rosa, I. G., & Cava, A. 2009, *ApJ*, 692, L118
- Trujillo, I., Ferreras, I., de La Rosa, I. G., 2011, *MNRAS*, 415, 3903
- Valentinuzzi, T., et al., 2010, *ApJ*, 712, 226
- van de Sande, J., et al., 2011, *ApJ*, 736, L9
- van der Wel, A., Franx, M., van Dokkum, P. G., Rix, H.-W., Illingworth, G. D., & Rosati, P. 2005, *ApJ*, 631, 145
- van der Wel, A., Holden, B. P., Zirm, A. W., Franx, M., Rettura, A., Illingworth, G. D., & Ford, H. C. 2008, *ApJ*, 688, 48
- van der Wel, A. et al., 2011, *ApJ*, 730, 38
- van Dokkum, P. G., et al. 2008, *ApJ*, 677, L5
- van Dokkum, P. G., et al. 2010, *ApJ*, 709, 1018
- Vazdekis, A., Sánchez-Blázquez, P., Falcón-Barroso, J., Cenarro, A. J., Beasley, M. A., Cardiel, N., Gorgas, J. & Peletier, R. F., 2010, *MNRAS*, 404, 1639
- Zirm, A. W., et al. 2007, *ApJ*, 656, 66

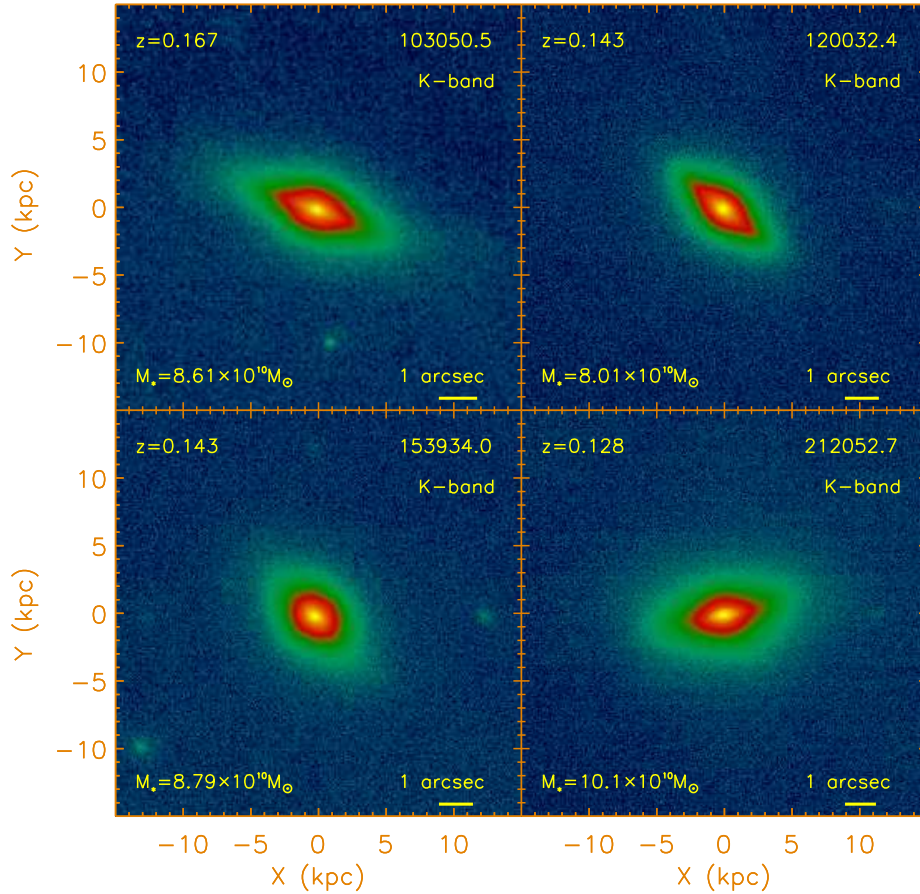


FIG. 1.— K-band Gemini high resolution (FWHM $\sim 0''.2$) imaging of four nearby ($z\sim 0.15$) massive compact galaxies. Listed on each figure is the galaxy name, its stellar mass and its spectroscopic redshift. The solid line indicates 1 arcsec angular size.

TABLE 1
GALAXY SAMPLE AND NIRI/ALTAIR OBSERVATIONS.

Name	R.A. (J2000)	Dec (J2000)	Observing date (UT)	Total Exposure time (sec)	Airmass	Zero Point (AB mag)	K mag (AB mag)
(1)	(2)	(3)	(4)	(5)	(6)	(7)	(8)
SDSS J103050.53+625859.8	10 30 50.53	+62 58 59.8	2010-02-28	3540	1.406	24.86	16.63
SDSS J120032.46+032554.1	12 00 32.46	+03 25 54.1	2010-06-05	1620	1.106	24.85	16.06
SDSS J153934.07+441752.2	15 39 34.07	+44 17 52.2	2010-05-04	3660	1.281 ^a	24.91 ^b	16.04
SDSS J212052.74+110713.1	21 20 52.74	+11 07 13.1	2010-06-04				
			2010-05-22	3780	1.230	24.90	16.24

NOTE. — Table description - column (1): galaxy name; column (2) and (3): Right Ascension (hours, minutes and seconds) and Declination (degrees, minutes and seconds); column (4): Date of observation in UT; column (5): the number of images and individual exposure time; column (6): effective airmass; column (7): Derived zero point in the AB system; column (8): K-band galaxy magnitude

^a Average airmass from two nights

^b Average Zero Point for two nights: Night 1: 24.90 mag, Night 2: 24.91 mag

TABLE 2
NEARBY MASSIVE COMPACT GALAXIES PROPERTIES

Name	M_* ($10^{10}M_{\odot}$)	R_e (arcsec)	Sérsic index	b/a	R_e (kpc)	Redshift	σ (km/s)
SDSS J103050.53+625859.8	8.61	0.45 ± 0.07	2.20 ± 0.24	0.36	1.23 ± 0.18	0.167	196 ± 16
SDSS J120032.46+032554.1	8.01	0.53 ± 0.08	3.55 ± 0.39	0.32	1.33 ± 0.20	0.143	266 ± 23
SDSS J153934.07+441752.2	8.79	0.38 ± 0.06	2.18 ± 0.24	0.47	0.95 ± 0.14	0.143	285 ± 40
SDSS J212052.74+110713.1	10.10	0.59 ± 0.09	2.66 ± 0.29	0.28	1.35 ± 0.20	0.128	223 ± 12

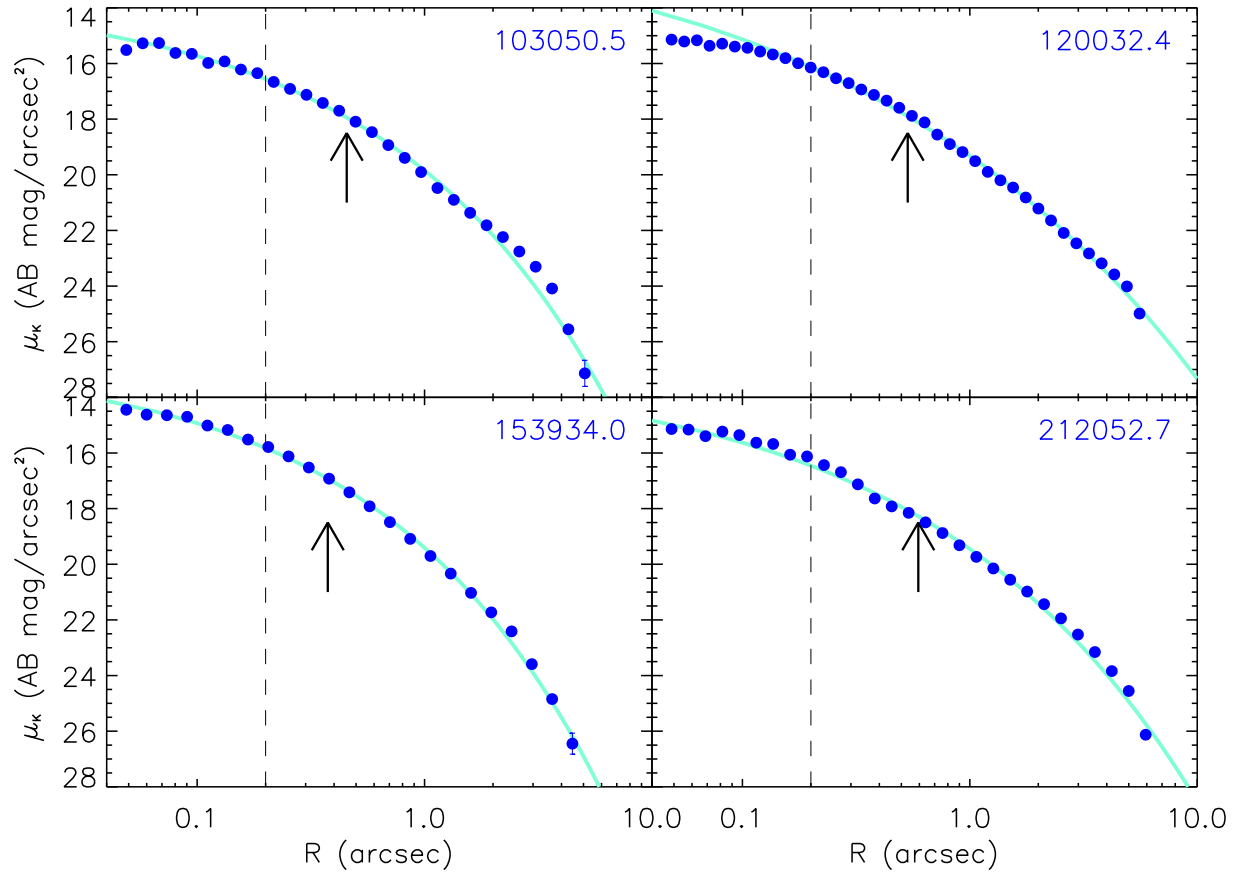


FIG. 2.— K-band surface brightness profiles of our sample of nearby massive compact galaxies (blue points). The soft blue lines are the best Sérsic fit to the data. The vertical line shows a FWHM PSF of 0.2 arcsec (the typical resolution of our images). The depth and high resolution of our images allow us to explore the profiles of our sample around 12 magnitudes in range, reaching many (~ 8) times the effective radii of these objects. The arrows indicate the position of the effective radii of our galaxies.

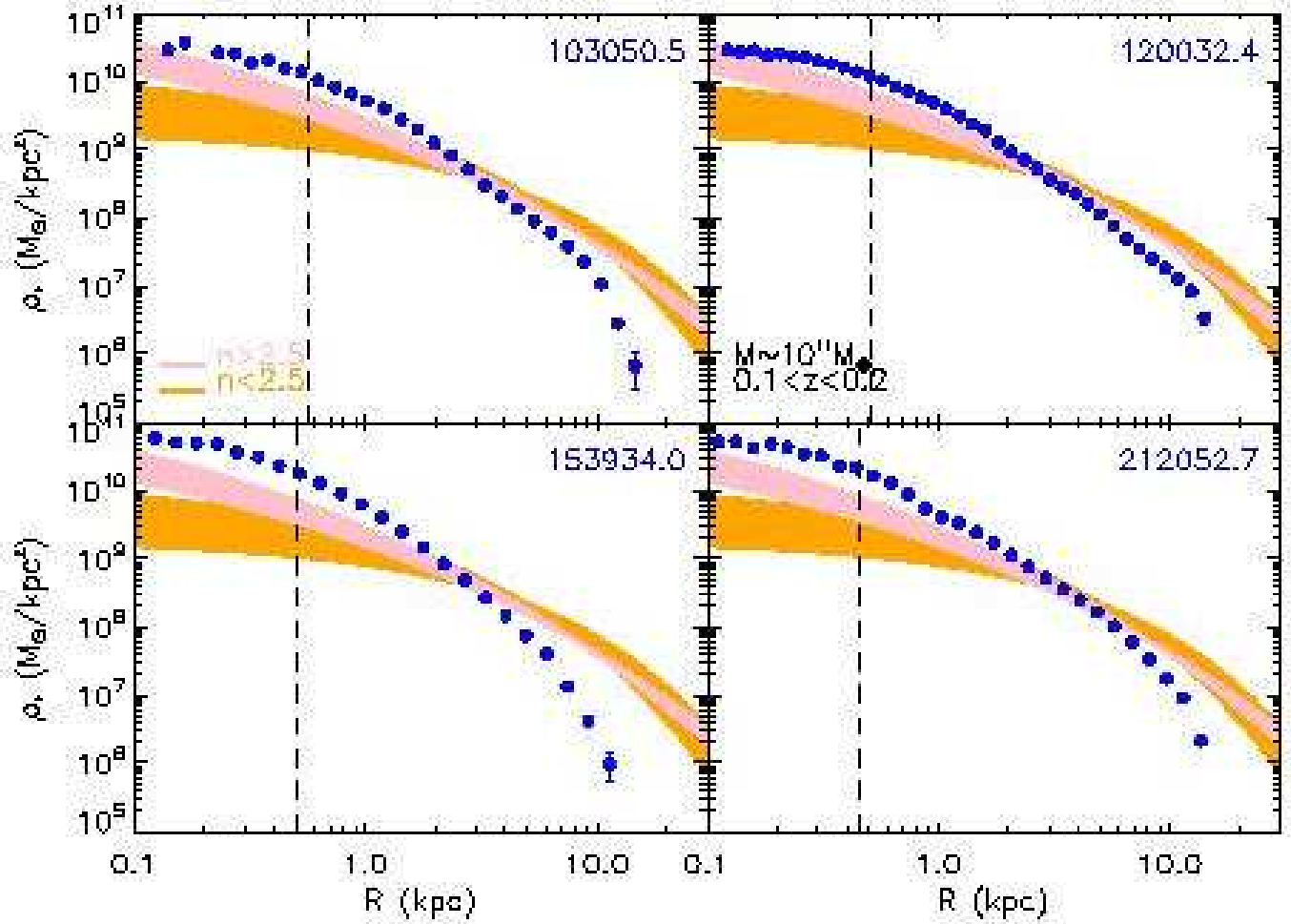


FIG. 3.— Stellar surface mass density profiles of our sample of nearby massive compact galaxies (blue points). The observed profiles of the compact massive galaxies are compared with SDSS DR7 stellar mass density profiles of $M_* \sim 10^{11} M_\odot$ and $0.1 < z < 0.2$ disk-like galaxies (Sérsic index $n < 2.5$; orange region) and with spheroid-like (Sérsic index $n > 2.5$; pink region) galaxies. The vertical line shows the equivalent size in kpc of a FWHM PSF of 0.2 arcsec. The depth and high resolution of our images allow us to explore the profiles of our sample galaxies from 0.1 to 20 kpc.

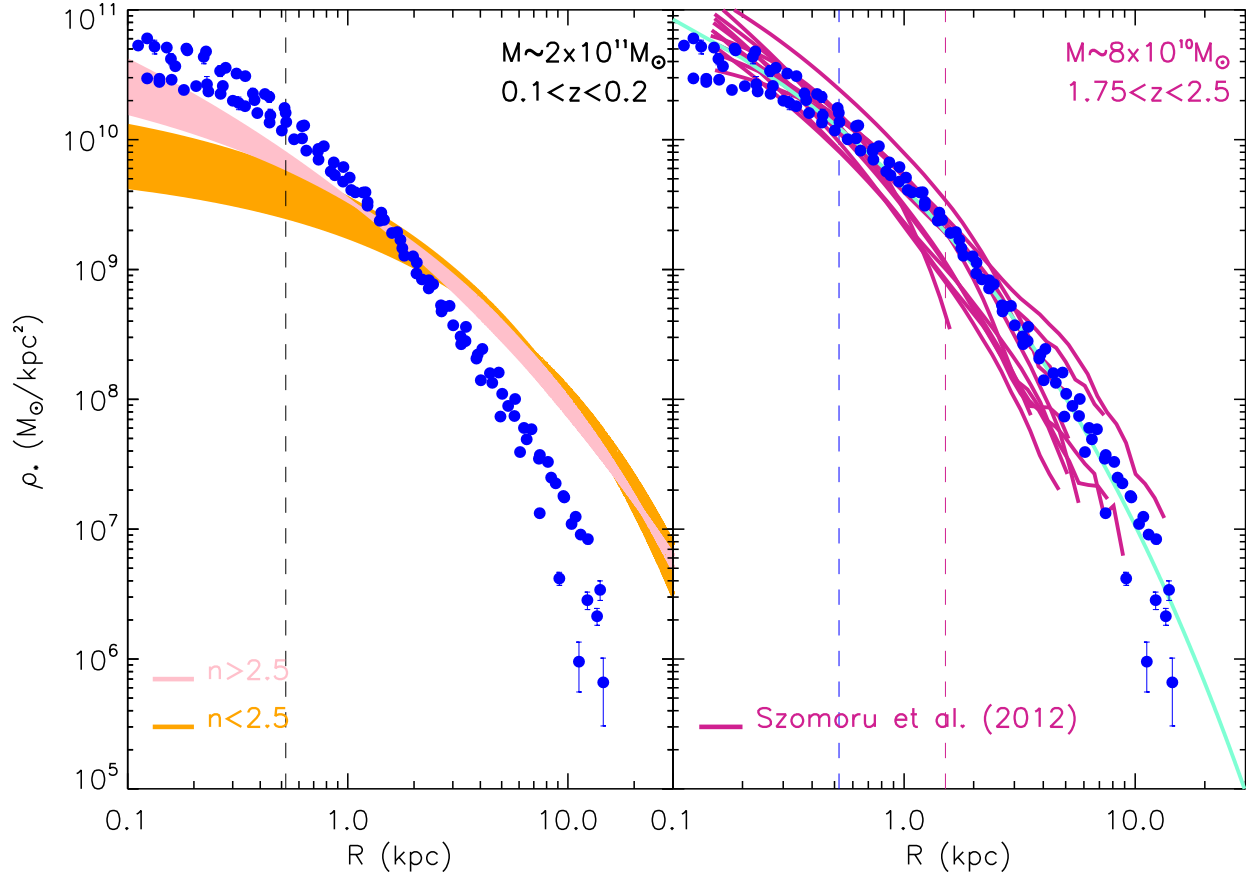


FIG. 4.— Stellar surface mass density profiles of our sample of nearby massive compact galaxies (blue points). *Left Panel* The observed profiles of the compact massive galaxies are compared with the stellar mass density profiles of SDSS DR7 $M_* \sim 2 \times 10^{11} M_\odot$ and $0.1 < z < 0.2$ disk-like galaxies (Sérsic index $n < 2.5$; orange region) and with spheroid-like (Sérsic index $n > 2.5$; pink region) galaxies. The vertical line shows the equivalent size in kpc of a FWHM PSF of 0.2 arcsec at $z=0.15$. *Right Panel* The nearby massive compact galaxies profiles are compared with profiles $z \sim 2$ massive compact galaxies (violet lines) of the same stellar mass (Szomoru et al. 2012). The agreement is remarkable. The dashed vertical blue line shows the equivalent size in kpc of a FWHM PSF of 0.2 arcsec at $z=0.15$ (our Gemini PSF) and the red vertical line the equivalent size in kpc of a FWHM PSF of 0.18 arcsec at $z=1.9$ (HST WFC3 PSF).